

Inactivation of *Bap1* Cooperates with Losses of *Nf2* and *Cdkn2a* to Drive the Development of Pleural Malignant Mesothelioma in Conditional Mouse Models



Anna-Mariya Kukuyan¹, Eleonora Sementino¹, Yuwaraj Kadariya¹, Craig W. Menges¹, Mitchell Cheung¹, Yinfei Tan¹, Kathy Q. Cai², Michael J. Slifker³, Suraj Peri³, Andres J. Klein-Szanto², Frank J. Rauscher III⁴, and Joseph R. Testa¹

Abstract

Pleural malignant mesothelioma is a therapy-resistant cancer affecting the serosal lining of the thoracic cavity. Mutations/deletions of *BAP1*, *CDKN2A*, and *NF2* are the most frequent genetic lesions in human malignant mesothelioma. We introduced various combinations of these deletions in the pleura of conditional knockout (CKO) mice, focusing on the contribution of *Bap1* loss. While homozygous CKO of *Bap1*, *Cdkn2a*, or *Nf2* alone gave rise to few or no malignant mesotheliomas, inactivation of *Bap1* cooperated with loss of either *Nf2* or *Cdkn2a* to drive development of malignant mesothelioma in approximately 20% of double-CKO mice, and a high incidence (22/26, 85%) of malignant mesotheliomas was observed in *Bap1*; *Nf2*; *Cdkn2a* (triple)-CKO mice. Malignant mesothelioma onset was rapid in triple-CKO mice, with a median survival of only 12 weeks, and malignant mesotheliomas from these mice were consistently high-grade and invasive. Adenoviral-Cre treatment of normal mesothelial cells from *Bap1*; *Nf2*; *Cdkn2a* CKO mice, but not from mice with knockout of one

or any two of these genes, resulted in robust spheroid formation *in vitro*, suggesting that mesothelial cells from *Bap1*; *Nf2*; *Cdkn2a* mice have stem cell-like potential. RNA-seq analysis of malignant mesotheliomas from triple-CKO mice revealed enrichment of genes transcriptionally regulated by the polycomb repressive complex 2 (PRC2) and others previously implicated in known *Bap1*-related cellular processes. These data demonstrate that somatic inactivation of *Bap1*, *Nf2*, and *Cdkn2a* results in rapid, aggressive malignant mesotheliomas, and that deletion of *Bap1* contributes to tumor development, in part, by loss of PRC2-mediated repression of tumorigenic target genes and by acquisition of stem cell potential, suggesting a potential avenue for therapeutic intervention.

Significance: Combinatorial deletions of *Bap1*, *Nf2*, and *Cdkn2a* result in aggressive mesotheliomas, with *Bap1* loss contributing to tumorigenesis by circumventing PRC2-mediated repression of oncogenic target genes.

Introduction

Pleural malignant mesothelioma is an aggressive, treatment-resistant cancer, which is causally related to asbestos exposure. Early cytogenetic and deletion mapping studies had uncovered several prominent sites of chromosomal loss in human pleural malignant mesothelioma, including 3p21, 9p21, and 22q12, and these recurrent abnormalities often occurred in combination in a given tumor, suggesting a multistep pathogenetic process (1).

Alterations in the target tumor suppressor genes at two of these sites, that is, *CDKN2A* at 9p21 and *NF2* at 22q12, were first discovered more than two decades ago (2–6), whereas the identity of the crucial 3p21 gene in malignant mesothelioma remained a mystery until 2011, when *BAP1* was identified as the critical malignant mesothelioma tumor suppressor gene at this location (7, 8). In a recent comprehensive study as part of The Cancer Genome Atlas, somatic genetic alterations of *BAP1*, *NF2*, and *CDKN2A* were observed in combination in 25 of 74 (34%) pleural malignant mesotheliomas (9).

The alterations of *CDKN2A* involve heterozygous or homozygous deletions of all or part of the locus (2). Abnormalities of *NF2* in malignant mesothelioma frequently are biallelic, consisting of both an inactivating mutation and loss of the second allele (10). Biallelic losses of *CDKN2A* have been documented in approximately 40% of primary malignant mesotheliomas (7) and up to 90% of malignant mesothelioma cell lines (2), whereas inactivating *NF2* mutations have been reported in 20%–55% of cases (5–7, 10). Using Sanger sequencing, somatic inactivating mutations of *BAP1* were initially reported in 20%–25% of sporadic malignant mesotheliomas (7, 8), but more recent studies with other sequencing platforms such as targeted next generation sequencing and multiplex ligation-dependent probe

¹Cancer Biology Program, Fox Chase Cancer Center, Philadelphia, Pennsylvania. ²Histopathology Facility, Fox Chase Cancer Center, Philadelphia, Pennsylvania. ³Bioinformatics and Biostatistics Facility, Fox Chase Cancer Center, Philadelphia, Pennsylvania. ⁴Wistar Institute, Philadelphia, Pennsylvania.

Note: Supplementary data for this article are available at Cancer Research Online (<http://cancerres.aacrjournals.org/>).

Corresponding Author: Joseph R. Testa, Fox Chase Cancer Center, 333 Cottman Avenue, Philadelphia, PA 19111. Phone: 215-728-2610; Fax: 215-214-1619; E-mail: joseph.testa@fccc.edu

Cancer Res 2019;79:4113–23

doi: 10.1158/0008-5472.CAN-18-4093

©2019 American Association for Cancer Research.

amplification have uncovered *BAP1* alterations in approximately 60% of cases, with a preponderance of exonic deletions (11).

The *CDKN2A* locus encodes the tumor suppressors p16INK4A and p14ARF, which regulate the Rb and p53 cell-cycle pathways, respectively. In malignant mesothelioma, the deleted region of *CDKN2A* typically includes exon 2 (2), which encodes portions of p16INK and p14ARF, and is thus predicted to affect both Rb and p53 pathways. Reexpression of p16INK4A in malignant mesothelioma cells results in cell-cycle arrest and tumor suppression/regression (12), while reexpression of p14ARF in malignant mesothelioma cells induces G₁ arrest/apoptosis (13). Underscoring the relevance of *Cdkn2a* to malignant mesothelioma pathogenesis, heterozygous *Cdkn2a* knockout mice treated with asbestos develop malignant mesothelioma at a significantly accelerated rate compared with asbestos-treated wild-type (WT) littermates (14). In addition, mice deficient for both p16INK4a and p19Arf exhibit enhanced asbestos-induced malignant mesothelioma formation relative to mice deficient for either p16INK4a or p19Arf alone (14).

Loss of the *NF2* product, merlin, in malignant mesothelioma leads to cell-cycle progression by upregulation of cyclin D1 both transcriptionally (15) and posttranscriptionally via activation of mTORC1 (16). *NF2* also inhibits Pak and FAK signaling, which play key roles in cell migration and spreading, respectively, and inactivation of *NF2* in malignant mesothelioma cells promotes invasiveness and spreading (17, 18). *Nf2*^{+/-} mice treated with asbestos develop malignant mesothelioma at an accelerated rate compared with asbestos-treated WT mice, suggesting that merlin inactivation contributes significantly to malignant mesothelioma development (4, 19, 20). Moreover, mice with heterozygous losses of both *Nf2* and *Cdkn2a* show further acceleration of asbestos-induced malignant mesothelioma, with resulting tumors exhibiting increased cancer stem cells and enhanced tumor spreading capability compared with that observed in mice with losses of only one or the other of these genes (21). Similarly, conditional knockout (CKO) mice harboring homozygous deletions of both *Nf2* and *p16INK4a/p19Arf* in the mesothelial lining of the thoracic cavity developed a high incidence of pleural malignant mesothelioma that showed increased pleural invasion compared with *Nf2;Tp53* CKO mice (20).

BRCA1-associated protein-1 (BAP1) was discovered as an ubiquitin hydrolase that associates with the RING finger domain of BRCA1 and enhances BRCA1-mediated inhibition of breast cancer cell growth (22). BAP1 interacts with ASXL family members to form the polycomb group (PcG) repressive deubiquitinase (PR-DUB) complex involved in stem cell pluripotency and other developmental processes (23). BAP1 also interacts with and deubiquitinates the transcriptional regulator host cell factor 1 (HCF1) (24). Importantly, BAP1 has been shown to form complexes with numerous transcription factors and cofactors, including transcription factor YY1 (25). The BAP1 ubiquitin carboxyl hydrolase activates transcription in an enzyme-dependent manner and regulates the expression of a variety of genes involved in numerous processes, including cell proliferation, DNA damage and inflammatory responses, metabolism, and various mechanisms of cell death (24, 26–29). In animal models, asbestos exposure induces a significant increase in the incidence of malignant mesothelioma in heterozygous *Bap1*-mutant mice as compared with asbestos-exposed WT littermates (30, 31).

Malignant mesothelioma patients with germline *BAP1* mutations have an improved long-term survival compared with malig-

nant mesothelioma patients without such heritable variants (32, 33). However, it remains unclear whether somatic *BAP1* mutations/deletions are associated with a poor prognosis in sporadic malignant mesothelioma, as is the case in uveal melanoma and renal cell carcinoma (34, 35). While most human malignant mesotheliomas exhibit somatic alterations of *BAP1*, *NF2*, and/or *CDKN2A*, currently it is not known whether inactivation of *BAP1* cooperates with loss of *NF2* and/or *CDKN2A* to drive a more aggressive malignant mesothelioma phenotype. Here, we address these questions experimentally using CKO models.

Materials and Methods

Mouse strains and genotyping

All mouse studies were performed in accordance with a protocol approved by the Fox Chase Cancer Center (FCCC) Institutional Animal Care and Use Committee. *Nf2^{flf};Cdkn2a^{flf}* mice in FVB/N genetic background (20), a gift from Anton Berns (Netherlands Cancer Institute, Amsterdam, The Netherlands), were maintained in our laboratory in a mixed FVB/N x 129/Sv background. The LoxP sites in the *Cdkn2a* locus of these mice permit excision of exon 2, which results in inactivation of both p16INK4a and p19Arf.

Bap1^{flf} mice in FVB/N background were developed in our laboratory using zinc finger nuclease (ZFN) technology, with the assistance of the FCCC Transgenic Mouse Facility. Custom ZFNs targeting *Bap1* were designed and validated in mammalian cells by Sigma-Aldrich. A pair of ZFNs was identified that binds to and cuts within a site in intron 5 of *Bap1* with high efficiency and specificity. We then designed a donor DNA construct containing LoxP sites in introns 6 and 7 (Fig. 1A), such that upon adenovirus-mediated expression of Cre recombinase there is deletion of exon 7 of *Bap1*. The ZFN mRNAs and donor DNA were injected into the pronucleus of one-cell embryos of FVB/N mice, and embryos were then transferred into pseudo-pregnant females. DNA from pups was analyzed for correct targeting by PCR amplification of the gene and sequencing. Three founder mice with LoxP sites integrated in the *Bap1* locus were identified, one of which was used for experiments reported here. Representative examples of genotyping of DNA from *Bap1* CKO mice are shown in Fig. 1B.

In addition to *Bap1^{flf}*, *Nf2^{flf}*, and *Cdkn2a^{flf}* mice, these CKO animals were crossed to generate cohorts with the following genotypes: *Bap1^{flf};Nf2^{flf}*, *Bap1^{flf};Cdkn2a^{flf}*, *Nf2^{flf};Cdkn2a^{flf}* and *Bap1^{flf};Nf2^{flf};Cdkn2a^{flf}*. The following primers and annealing temperatures were used for genotyping: *Bap1^{flf}* 1063: 5'-CCC TGA GAC CCA GAA AAT CA-3', Tm = 54.3°C; *Bap1^{flf}* 1228: 5'-GGG AGG CTC TTT GAA TTG GA-3', Tm = 54.9°C; *Nf2^{flf}* 1048: 5'-CTT CCC AGA CAA GCA GGG TTC-3', Tm = 58.0°C; *Nf2^{flf}* 1049: 5'-GAA GGC AGC TTC TTC CTT AAG TC-3', Tm = 53.2°C; *Cdkn2a^{flf}* 1025: 5'-GCA GTG TTG CAG TTT GAA CCC-3', Tm = 57.4°C; and *Cdkn2a^{flf}* 1026: 5'-TGT GGC AAC TGA TTC AGT TGG-3', Tm = 55.8°C.

Adeno-Cre injections

Ad5CMVCre (Adeno-Cre) virus was obtained from the Viral Vector Core of the University of Iowa (Iowa City, IA). Mice 8–12 weeks of age were injected intrathoracically (20), specifically intrapleurally, with Adeno-Cre virus (50 µL of 3–6 × 10¹⁰ PFU), with approximately equal numbers of mice of each gender in each cohort. Mice were monitored daily and were euthanized upon visible signs of distress, including extreme fatigue, labored

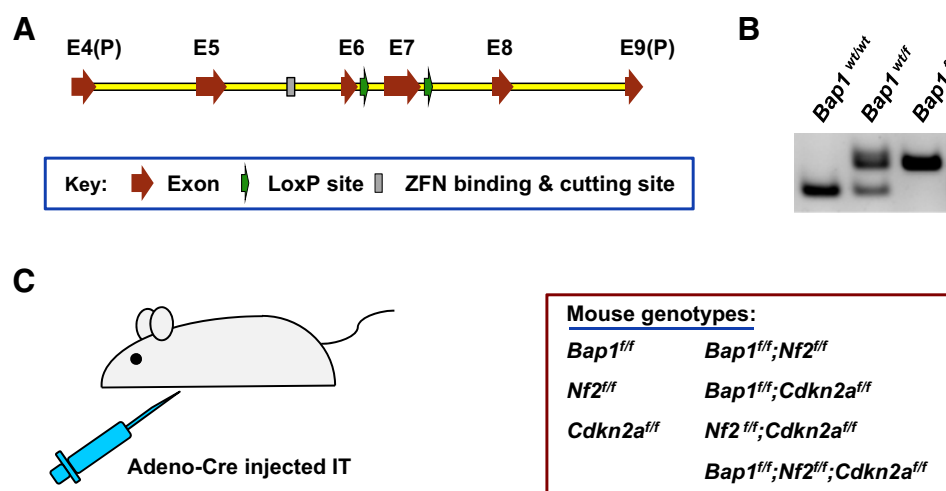


Figure 1.

Generation of *Bap1* CKO mouse with ZFN technology and experimental schema used for crosses with other CKO mice. **A**, Schematic drawing of *Bap1* LoxP donor DNA sequence. Donor DNA contains region spanning part of exon 4, E4(P), to part of exon 9, E9(P). LoxP sites were inserted into introns 6 and 7. A pair of ZFNs was identified that binds to and cuts within a site in intron 5 of *Bap1* with high efficiency and specificity. A donor DNA construct was then designed that contained two LoxP sites, one in intron 6 and one in intron 7, as shown, such that expression of Adeno-Cre in the mouse mesothelial cell lining of the pleural cavity excised exon 7 of *Bap1*. **B**, Genotyping of DNA from wild-type (wt) mouse as well as heterozygous (wt/f) and homozygous (f/f) *Bap1* CKO mice. **C**, Strategy used to homozygously excise *Bap1*, *Nf2*, and/or *Cdkn2a* via intrathoracic injection of Adeno-Cre virus in mice with the various genotypes is shown. IT, intrathoracically.

breathing, or when mice exhibited a 10% change in body weight. Tissues of all organs of the pleural and peritoneal cavities were collected from sacrificed mice and tumor specimens were subjected to histopathologic assessment. Portions of tumors were also saved in both O.C.T. Compound and RNAlater Solution (Thermo Fisher Scientific) and immediately frozen at -80°C .

Tumor histopathology, IHC, and RT-PCR analysis

The histopathologic procedures used are essentially the same as described previously (23). In summary, after paraffin embedding, sectioning, and deparaffinization, hematoxylin and eosin-stained sections were used for histopathologic evaluation, and unstained sections were used for IHC. For IHC, sections were subjected to heat-induced epitope retrieval using citrate buffer (pH 6.0) for 20 minutes.

Malignant mesotheliomas were diagnosed by two independent pathologists (A.J. Klein-Szanto and K.Q. Cai). To confirm the diagnosis of malignant mesothelioma, IHC was performed for various malignant mesothelioma markers, including mesothelin, detected with Mesothelin antibody PA5-79698 (Invitrogen), and cytokeratin 8, detected with TROMA-1 antibody (DSHB, University of Iowa, Iowa City, IA). In addition, reverse transcription-PCR (RT-PCR) analysis was also performed to analyze malignant mesothelioma markers, including *Wt1*, *Msln* (mesothelin), and *Krt18/19* (cytokeratin 18/19). RT-PCR analysis for *Msln* used primers 5'-ATCAAGACATTCCTGGGTGGG-3' and 5'-CGGTAAAGCTGGGAGCAGAG-3'. Primers for other malignant mesothelioma markers have been described previously (4). To assess cell proliferation, IHC staining was performed with antibodies for Ki-67 (Dako/Agilent).

Immunoblot analysis and antibodies

Immunoblots were prepared with 30–50 μg of protein lysate per sample, as described previously (21). Anti-Bap1

antibody (A302-243, 1:2,000) was purchased from Bethyl Laboratories. Anti-p19Arf (5-C3-1, sc-32748 1:1,000), anti-Gapdh (6C5, sc-32233, 1:50,000), and anti- β -actin (C4, sc-47778, 1:50,000) were from Santa Cruz Biotechnology; anti-Nf2 (D1D8, #6995S, 1:1,000), anti-total-Akt (#9272S, 1:1,000), and anti-P-Akt, Ser473 (D9E XP, #4060, 1:1,000) were from Cell Signaling Technology and anti-p16 (ab189034 1:1,000) was from Abcam. Immunoblots were imaged using Immobilon Western Chemiluminescent HRP Substrate (EMD Millipore; P90720 catalog no. WBKLS0500).

Spheroid growth assay

Primary normal mesothelial cells were isolated from individual CKO mice, 10–12 weeks of age, with each of the following genotypes: *Bap1^{f/f}*, *Nf2^{f/f}*, *Cdkn2a^{f/f}*, *Bap1^{f/f};Nf2^{f/f}*, *Bap1^{f/f};Cdkn2a^{f/f}*, *Nf2^{f/f};Cdkn2a^{f/f}*, and *Bap1^{f/f};Nf2^{f/f};Cdkn2a^{f/f}*. The mesothelial cells were isolated by sacrificing animals and adding trypsin (0.25% Trypsin-EDTA, Gibco, 25200-056) to the peritoneal cavity, according to the method of Bot and colleagues (36). Normal mesothelial cells at passage 2 were then seeded in 6-well plates (Thermo Fisher BioLite 6-well Multidish, catalog no. 130184) and treated with 4×10^{10} PFU/mL of either control Ad5CMVempty (Adeno-CMV) or Adeno-Cre virus for 1 hour. Cells were then washed in PBS, cultured in normal mesothelial media (34) for 72 hours, and trypsinized. Next, 5,000 mesothelial cells were seeded in each well of a 6-well nonadherent plate (Corning, Costar) in serum-free DMEM/F12 media supplemented with B27, EGF (10 ng/mL), basic FGF (10 ng/mL), and penicillin/streptomycin, as described previously (21). The experiment was performed in triplicate for each cell genotype. Spheroids were photographed using light microscopy after 9 days of culture.

RNA-seq analysis

Tumor RNA was isolated in TRIzol and purified with RNeasy columns (Qiagen). RNA-seq was performed with a HiSeq Sequencer and the following reagents: TruSeq Stranded mRNA Library, HiSeq Rapid SR Cluster, and HiSeq Rapid SBS v2 kits (Illumina). Stranded mRNA-seq libraries were prepared according to Illumina's product guide. First-strand cDNA was synthesized using SuperScript II reverse transcriptase (Thermo Fisher Scientific) and random primers at 42°C for 15 minutes, followed by second strand synthesis at 16°C for 1 hour. Adapters with Illumina P5/P7 sequences and indices were ligated to cDNA fragments, and libraries were pooled and loaded onto the sequencer. Fastq files were aligned to the mm10 mouse genome using TopHat2. Raw sequence counts for each gene were produced with HTseq (<https://htseq.readthedocs.io>) and differentially expressed genes were identified by DESeq2 (37). RNA-seq heatmaps were constructed from $\log_2(x+1)$ -transformed counts/million, standardized across rows, using the "heatmap.2" function from the R *gplots* library. Raw sequencing data have been deposited in the GEO repository (accession number GSE131942).

Gene-set enrichment analysis

For functional enrichment analysis, genes identified as differentially expressed by DESeq2 with nominal $P < 0.5$ were ranked by fold-change and mapped to human genes using R *biomaRt* (38). These genes were then analyzed using the GSEAPreranked method of Gene Set Enrichment Analysis (GSEA; ref. 39) (with "classic" enrichment statistic) applied to the curated (c2) and Gene Ontology gene sets from the Molecular Signature Database (MSigDB). Confirmation of differentially expressed genes was performed by quantitative RT-PCR analysis; Taqman (Thermo Fisher Scientific) assay IDs used for 13 genes validated by RT-PCR analysis are shown in Supplementary Table S1.

Results

Temporal intrathoracic inactivation of *Bap1* together with *Nf2* and/or *Cdkn2a* results in malignant mesothelioma and other tumors

Injection of Adeno-Cre virus into the pleural space of Rosa26 LacZ reporter (R26R) mice has been previously reported to result in efficient β -galactosidase expression in the mesothelial cell lining of the chest cavity (20). Locotemporal expression of Cre recombinase by intrathoracic injection of Adeno-Cre was used to induce mesothelial cell-specific loss of *Bap1*, *Nf2*, and/or *Cdkn2a* in homozygous single-gene CKO mice and in homozygous compound CKO mice. The injection scheme used for the CKO mice is depicted in Fig. 1C. Tumors that arose in most mouse cohorts were mainly malignant mesotheliomas, although other neoplasms were also observed (Table 1).

In the cohorts of mice with homozygous knockout of a single gene only, few malignant mesotheliomas were seen. Among 32 *Bap1*^{fl/fl} CKO mice injected intrathoracically with Adeno-Cre, a slow growing, well-differentiated malignant mesothelioma was identified in a single animal 45 weeks after injection. Interestingly, this malignant mesothelioma acquired loss of *Nf2* and p16Ink4a expression during tumor formation (Supplementary Fig. S1A). As expected, this tumor showed *Bap1* loss-related deficient deubiquitination activity; and con-

Table 1. Summary of tumors observed in homozygous conditional knockout mice arising after intrathoracic injection of Adeno-Cre

Genotype ^a	<i>Bap1</i> ^{fl/fl}	<i>Bap1</i> ^{fl/fl} ; <i>Nf2</i> ^{fl/fl}	<i>Bap1</i> ^{fl/fl} ; <i>Cdkn2a</i> ^{fl/fl}	<i>Nf2</i> ^{fl/fl} ; <i>Cdkn2a</i> ^{fl/fl}	<i>Bap1</i> ^{fl/fl} ; <i>Nf2</i> ^{fl/fl} ; <i>Cdkn2a</i> ^{fl/fl}
No. of mice injected	32	42	27	24	26
MM	1 (3.1%)	7 (16.6%)	6 (22.2%)	15 ^c (62.5%)	22 (84.6%)
Epithelioid	0	0	0	0	0
Mixed (biphasic)	0	6	1	4	8
Sarcomatoid	1	1	5	11	14
Lymphoma	1	0	0	0	0
Adenocarcinoma	2	0	2	0	0
HCC/ICC	0	28 ^{c,d}	0	2 ^e	0
Hemangiocarcinoma	0	0	2	0	0
Other causes of death ^b	29	10	17	9	4

Abbreviation: MM, malignant mesothelioma.

^aIn the other two single-gene CKO mouse cohorts, malignant mesothelioma was observed in 0 of 12 *Cdkn2a*^{fl/fl} mice and 2 of 15 *Nf2*^{fl/fl} mice, frequencies similar to a previous report (21).

^bMostly aged mice, with moribund animals often found to have plaques, bladder obstructions, or lymphoproliferative lesions.

^cOne mouse had both malignant mesothelioma and HCC, and two mice had malignant mesothelioma as well as HCC and ICC.

^dFourteen of the 28 mice had both HCC and ICC.

^eOne mouse had both malignant mesothelioma and ICC, and one mouse had malignant mesothelioma and HCC.

sistent with the acquired loss of *Nf2*/merlin, downstream Yap was not phosphorylated (Supplementary Fig. S1B). PCR analysis confirmed that losses of *Nf2* and *Cdkn2a* are acquired (Supplementary Fig. S1C). Malignant mesotheliomas were observed in 2 of 15 *Nf2*^{fl/fl} mice and 0 of 12 *Cdkn2a*^{fl/fl} mice injected with Adeno-Cre, results comparable with those reported in an earlier study (20).

Among the intrathoracically injected mice with homozygous inactivation of two genes, malignant mesotheliomas were observed in 7 of 42 (16.6%) *Bap1*;*Nf2* CKO mice, 6 of 27 (22.2%) *Bap1*;*Cdkn2a* CKO mice, and 15 of 24 (62.5%) *Nf2*;*Cdkn2a* CKO mice. The highest incidence of malignant mesothelioma (22/26, 84.6%) was observed in *Bap1*;*Nf2*;*Cdkn2a* triple-CKO mice. A summary of malignant mesothelioma incidence among *Bap1* CKO mice and mice with the various compound CKO genotypes is shown in Fig. 2A.

With regard to histologic subtype, notably no epithelioid malignant mesotheliomas were observed with any of the mouse genotypes. Sarcomatoid malignant mesotheliomas predominated in most cohorts, with the exception being *Bap1*;*Nf2* CKO mice, in which 6 of 7 MMs showed mixed (biphasic) histology.

Malignant mesothelioma latency varied between 21 and 40 weeks among the different compound double-CKO mice. A markedly shorter malignant mesothelioma latency, 12 weeks, was observed in *Bap1*;*Nf2*;*Cdkn2a* triple-CKO mice, a highly significant difference (log-rank test, $P < 0.0001$) from the 27 weeks observed for *Nf2*;*Cdkn2a* CKO mice or for any of the other compound double-CKO (DKO) mice. The malignant mesothelioma survival differences between the three cohorts with different DKO combinations were not statistically significant (Supplementary Table S2). Kaplan–Meier survival curves of intrathoracically injected mice that developed malignant mesothelioma are shown in Fig. 2B. In addition, malignant mesotheliomas from *Bap1*;*Nf2*;*Cdkn2a* CKO mice were

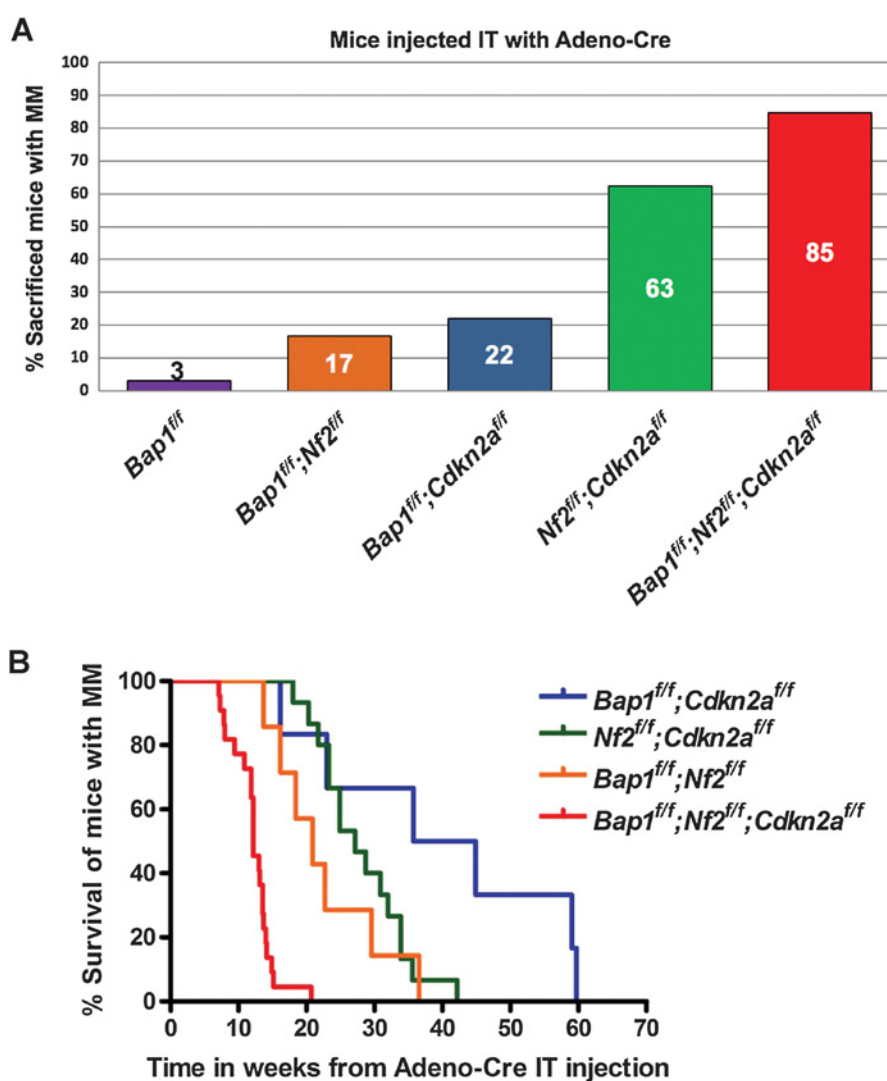


Figure 2.

Incidence and latency of pleural malignant mesothelioma (MM) in mouse cohorts with different genotypes following intrathoracic injections with Adeno-Cre virus. **A**, Incidence of malignant mesothelioma in the various CKO mouse groups. **B**, Tumor latency curves for malignant mesotheliomas arising after Adeno-Cre injections in mice with CKO of different combinations of *Bap1*, *Nf2*, and/or *Cdkn2a*. Kaplan-Meier curves depict survival of mice succumbing to malignant mesothelioma arising after intratumoral injections with Adeno-Cre. Note rapid development of malignant mesothelioma in triple-CKO mice, with the median survival being only 12 weeks, which was significantly different ($P < 0.0001$) from that of any of the other compound CKO mice. The survival differences between the other three DKO mouse cohorts were not statistically significant (Supplementary Table S2).

Genotype	% Mice with MM	Median survival in weeks
<i>Bap1^{fl/fl};Cdkn2a^{fl/fl}</i>	6/27 (22%)	40
<i>Bap1^{fl/fl};Nf2^{fl/fl}</i>	7/42 (17%)	21
<i>Nf2^{fl/fl};Cdkn2a^{fl/fl}</i>	15/24 (63%)	27
<i>Bap1^{fl/fl};Nf2^{fl/fl};Cdkn2a^{fl/fl}</i>	22/26 (85%)	12

consistently high-grade, very invasive, and highly proliferative tumors (Fig. 3A and B), whereas malignant mesothelioma morphology was generally more variable and less hypercellular with the other mouse genotypes. Immunoblotting confirmed the absence of expression of proteins encoded by conditionally knocked out genes *Bap1*, *Nf2*, and *Cdkn2a* (p16Ink4a and p19Arf) in 12 of 12 malignant mesotheliomas tested, and interestingly there was also acquired loss of expression of *Bap1* in 4 of 6 malignant mesotheliomas from *Nf2*;*Cdkn2a* CKO mice

(Fig. 4). We also assessed the status of Akt in these tumors, because Akt activation occurs frequently in human and murine malignant mesotheliomas (4). Akt activation was seen in all malignant mesotheliomas tested, as indicated by expression of phosphorylated (active) Akt (Fig. 4).

Besides malignant mesothelioma, various other tumor types were also seen in mice injected intrathoracically with Adeno-Cre (Table 1). Among mice with homozygous inactivation of *Bap1* alone in the thoracic cavity, 2 lung adenocarcinomas and 1

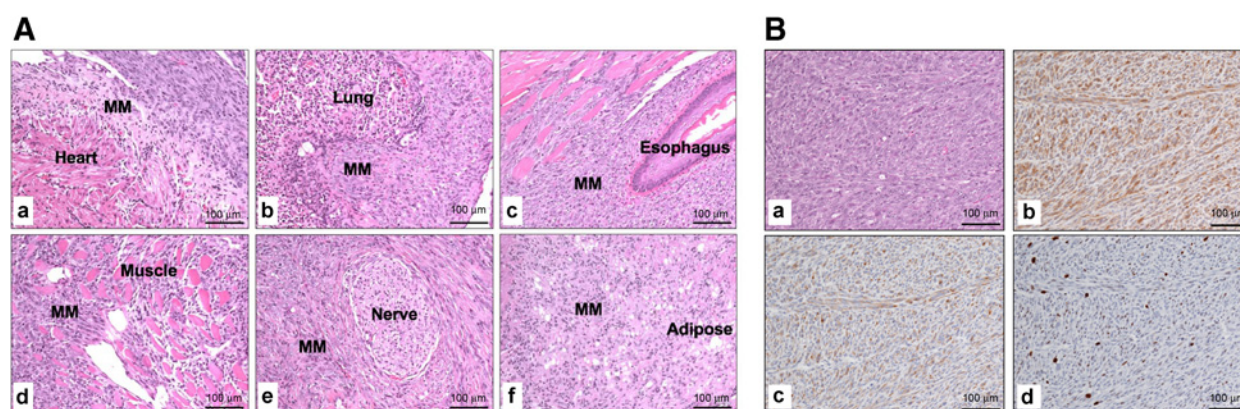


Figure 3. Histopathologic assessment of representative high-grade malignant mesotheliomas (MM) from *Bap1;Nf2;Cdkn2a* CKO mice. **A**, Histopathology of highly invasive, disseminated malignant mesothelioma that arose in a *Bap1;Nf2;Cdkn2a* CKO mouse following intrathoracic injection of Adeno-Cre. Note malignant mesothelioma invasion affecting multiple organs including the heart (a), lung (b), esophagus (c), skeletal muscle (d), nerve (e), and mediastinal adipose tissue (f). **B**, Serial sections of a malignant mesothelioma from a *Bap1;Nf2;Cdkn2a* CKO mouse showing hematoxylin and eosin staining (a), and IHC for mesothelin (b), cytokeratin 8 marker TROMA-1 (c), and nuclear proliferation marker Ki-67 (d).

lymphoma were seen. The remaining mice died of other age-related diseases, including bladder obstructions or lymphoproliferative diseases. Among the compound CKO mice, most notable was the cohort with inactivation of both *Bap1* and *Nf2*, which showed a high incidence (28/42, 66.7%) of hepatocellular carcinoma (HCC) and intrahepatic cholangiocarcinoma (ICC; Supplementary Fig. S2A and S2B, respectively), with these tumors generally arising later than malignant mesotheliomas in this cohort (median 35 weeks vs. 21 weeks, respectively). Altogether, 28 *Bap1;Nf2* CKO mice developed hepatic cancers, including 7 with HCC alone, 4 with ICC alone, 14 with both HCC and ICC, 1 with HCC and malignant mesothelioma, and 2 with HCC, ICC, and malignant mesothelioma.

Inactivation of three malignant mesothelioma driver tumor suppressor genes is sufficient to induce a stem cell-like phenotype in mesothelial cells

To assess the cooperativity of *Bap1*, *Nf2*, and *Cdkn2a* losses *in vitro*, we next used a spheroid growth assay. Primary normal mesothelial cells were isolated from *Bap1^{fl/fl}; Nf2^{fl/fl}; Cdkn2a^{fl/fl}*, *Bap1^{fl/fl}; Nf2^{fl/fl}*, *Bap1^{fl/fl}; Cdkn2a^{fl/fl}*, *Nf2^{fl/fl}; Cdkn2a^{fl/fl}*, and *Bap1^{fl/fl}; Nf2^{fl/fl}; Cdkn2a^{fl/fl}* mice. The mesothelial cells were then exposed to either control Adeno-CMV or Adeno-Cre virus for 1 hour, seeded in nonadherent plates in serum-free stem cell medium (21), and photographed after 9 days. There was little or no evidence of spheroid formation in cultured WT mesothelial cells or mesothelial cells with Adeno-Cre-induced homozygous inactivation of

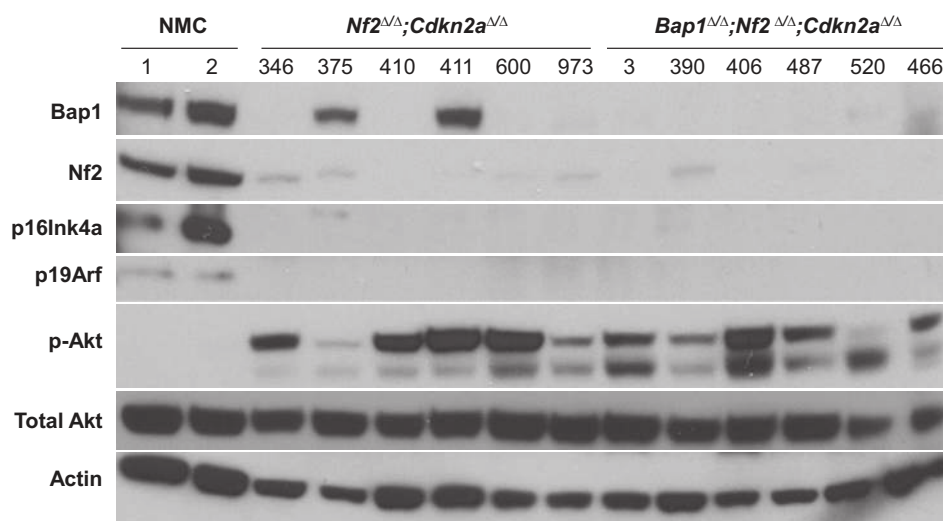
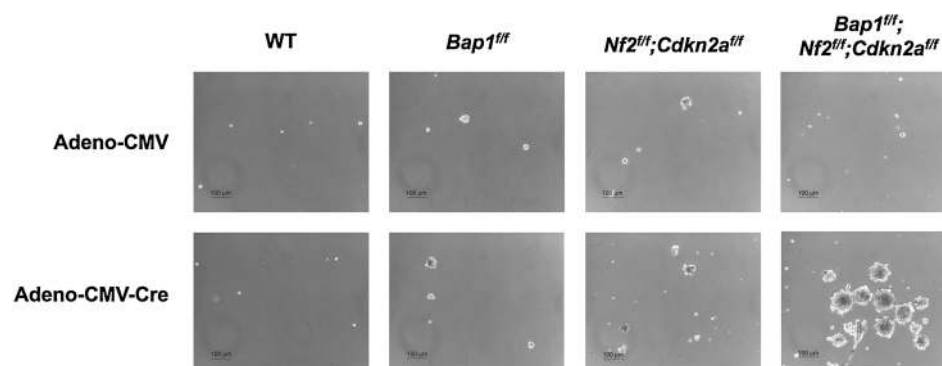


Figure 4. Western blot analysis of normal mesothelial cells (NMC) and malignant mesotheliomas from *Nf2;Cdkn2a* DKO and *Bap1;Nf2;Cdkn2a* TKO mice. Immunoblots confirm loss of expression of proteins encoded by conditionally knocked out genes *Bap1*, *Nf2*, and *Cdkn2a* (p16Ink4a and p19Arf) in all tumors. Acquired loss of expression of *Bap1* was also observed in 4 of 6 malignant mesotheliomas from *Nf2;Cdkn2a* DKO mice. Interestingly, this acquired loss of *Bap1* expression appears to have occurred at the posttranslational level, as these tumors showed no *Bap1* mutations, deletions, or loss of mRNA expression. Phosphorylated Akt, indicative of Akt activation, is seen in all malignant mesotheliomas shown.

Figure 5.

Ad5CMVCre virus-exposed normal mesothelial cells from *Bap1^{fl/fl};Nf2^{fl/fl};Cdkn2a^{fl/fl}* mice harbor more and much larger stem cell-like spheroids than do those from wild-type (WT), *Bap1^{fl/fl}*, and *Nf2^{fl/fl};Cdkn2a^{fl/fl}* mice. Equal numbers of normal mesothelial cells from mice with the various cited genotypes were seeded on nonadherent 6-well plates in stem cell media, and spheroids were photographed after 9 days.



one or various combinations of two tumor suppressor genes (representative examples shown in Fig. 5). In contrast, Adeno-Cre–treated mesothelial cells from *Bap1^{fl/fl};Nf2^{fl/fl};Cdkn2a^{fl/fl}* mice, that is, with inactivation of all three malignant mesothelioma driver genes, showed multiple large spheroids, indicative of stem cell features (Fig. 5).

RNA-seq analysis of malignant mesotheliomas from triple-CKO mice reveals enrichment of genes transcriptionally regulated by the polycomb repressive complex 2

Given the striking shift in malignant mesothelioma latency between *Bap1;Nf2;Cdkn2a* CKO mice and *Nf2;Cdkn2a* CKO mice, as well as the consistently more aggressive nature of malignant mesotheliomas from triple-CKO (TKO) mice, we performed RNA-seq analysis on malignant mesotheliomas from these two cohorts to shed light on the contribution of *Bap1* inactivation in this experimental setting. This analysis was carried out on all 6 malignant mesotheliomas from *Bap1;Nf2;Cdkn2a* CKO mice shown in Fig. 4 versus 2 malignant mesotheliomas from *Nf2;Cdkn2a* CKO mice in which *Bap1* expression was retained (tumors 375 and 411 in Fig. 4). Among 1,425 genes identified as differentially expressed with fold-change of at least 2 and false discovery rate (FDR) <1%, significantly fewer genes (628, 44%) were upregulated than downregulated ($P = 8.4 \times 10^{-6}$, exact binomial test) in malignant mesotheliomas from *Bap1*-deficient TKO mice versus *Bap1*-expressing malignant mesotheliomas from DKO mice. Functional enrichment analysis with GSEA identified several highly significant (family-wise error rate < 0.0005) curated gene sets. Prominent among the positively enriched gene sets were those related to writers of histone H3K27Me3, including PRC2 and SUZ12 (Fig. 6A), as well as genes participating in cell proliferation and transcription regulation involving ubiquitin signaling mediated by the Bap1–HCF1–YY1 complex, EED-related stem cell pluripotency, cytokine signaling, and cell adhesion; 100 of the top pathways differentially affected in malignant mesotheliomas from TKO versus DKO mice are presented in Supplementary Table S3. Considering that *Bap1* plays an important role in chromatin remodeling and transcriptional regulation (23–25), and the fact that many of the top differentially expressed genes were significantly enriched for PRC2 target genes (40), we decided to focus further on PRC2 targets here. A heatmap of genes differentially expressed in malignant mesotheliomas from triple-CKO mice versus malignant mesotheliomas from *Nf2;Cdkn2a* double-CKO mice is shown in Fig. 6B. Thirteen cancer-related genes were validated by RT-PCR analysis, 6 of which (e.g., *Ptchd1* and *Diras1*) are depicted in Fig. 6C and Supplementary Fig. S3. *Mmp9* protein was also shown to be overexpressed and activated

in malignant mesotheliomas from TKO mice versus those from DKO mice (Fig. 6D).

Discussion

In this investigation, our aim was to induce mesothelial cell-specific homozygous deletions of three tumor suppressor genes (*Bap1*, *Nf2*, and *Cdkn2a*) that have been implicated as major drivers of human malignant mesothelioma pathogenesis. While the majority of malignant tumors observed were malignant mesotheliomas, additional tumor types also resulted, possibly due to infection of other intrathoracic tissues or by passage of virus via blood vessels to the liver. Notably, HCCs and ICCs were very common later in life in *Bap1;Nf2* CKO mice but were observed in only two CKO mice with any of the other genotypes. Notably, liver-specific deletion of *Nf2* in the developing or adult mouse has been reported to promote a marked, progressive expansion of progenitor cells throughout the liver, with all surviving mice eventually developing both HCC and ICC (41). Interestingly, HCC and ICC were not seen in our *Bap1;Nf2;Cdkn2a* CKO cohort, perhaps because these mice succumbed to malignant mesothelioma before hepatic tumors could be detected.

Overall, the malignant mesotheliomas observed in our GEM cohorts generally showed morphologic features, IHC staining, and invasiveness similar to that of human sarcomatoid malignant mesotheliomas, with the exception being those observed in *Bap1;Nf2* CKO mice, in which 6 of 7 malignant mesotheliomas showed mixed (biphasic) histology that also was similar histologically to their human biphasic counterparts.

The Kaplan–Meier curves (Fig. 2B) indicate that homozygous inactivation of different combinations of *Bap1*, *Nf2*, and *Cdkn2a* affect malignant mesothelioma latency differently, with losses of all three genes profoundly accelerating tumor development. Specifically, *Bap1;Nf2;Cdkn2a* CKO mice bearing malignant mesothelioma showed much shorter tumor latency than mice in any compound double-CKO cohort. Moreover, malignant mesotheliomas from triple-CKO mice consistently appeared to be high grade, very invasive, hypercellular tumors, whereas malignant mesotheliomas from mice with other genotypes were more variable phenotypically. All malignant mesotheliomas observed in our study were sarcomatoid or biphasic, similar to what was reported by Jongsma and colleagues for mice with homozygously floxed conditional compound alleles that were injected intrathoracically with Adeno-Cre (20). For example, in their *Nf2;Cdkn2a* CKO mice, 31 malignant mesotheliomas were sarcomatoid, 13 had mixed histology, and only 1 was epithelioid (20). These investigators had speculated that the predominant epithelioid

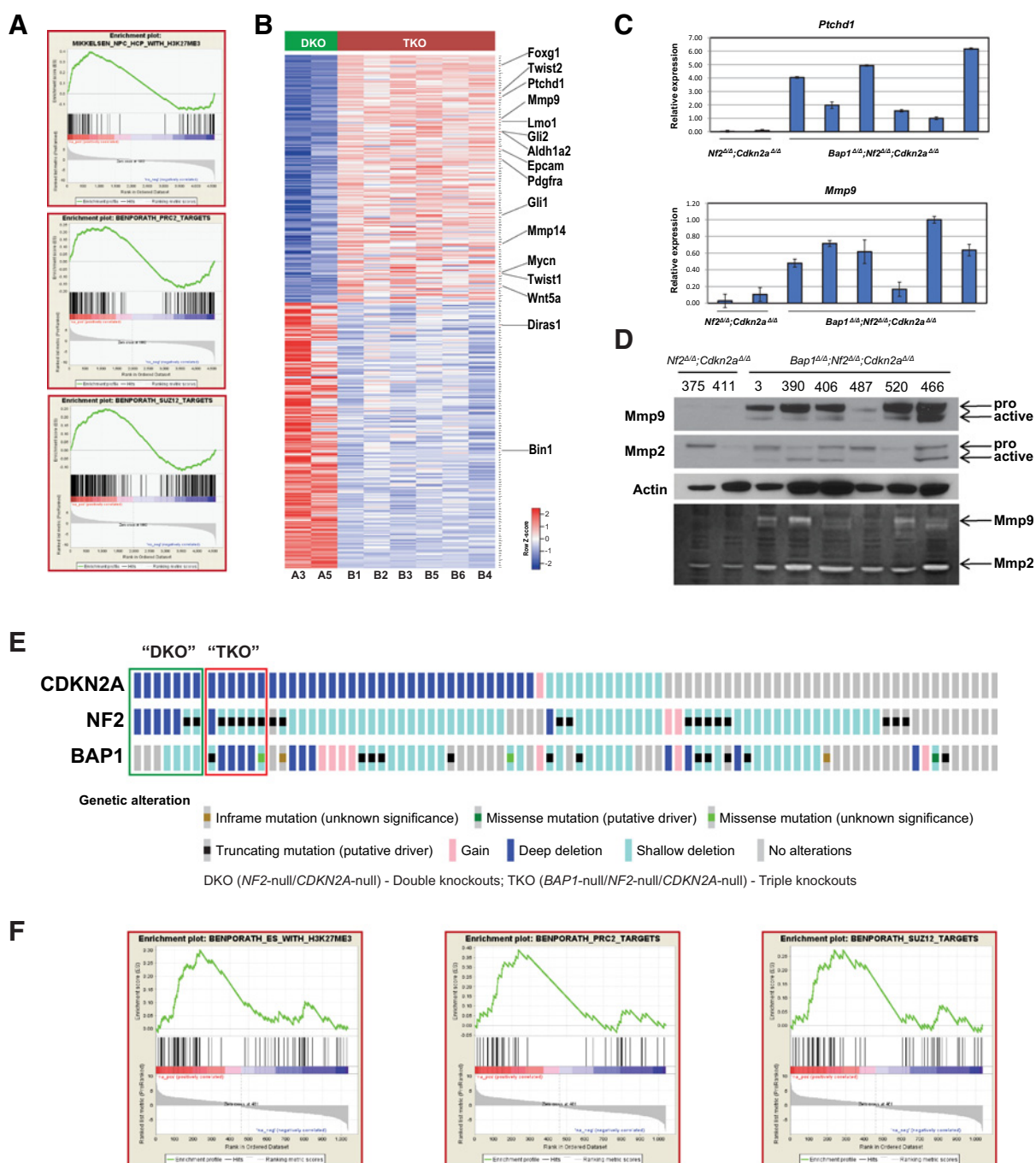


Figure 6. Heatmap and GSEA of same malignant mesotheliomas (MM; B1–B6) from *Bap1/Nf2/Cdkn2a* TKO mice shown in Fig. 4 versus two malignant mesotheliomas, A3 and A5 (375 and 411, respectively), from *Nf2/Cdkn2a* DKO mice retaining expression of *Bap1*. **A**, Gene enrichment plots of several gene sets differentially expressed in malignant mesotheliomas from TKO versus DKO mice. **B**, Top 400 PRC2 target genes differentially expressed with at least 2-fold change and FDR of <1%. Genes are ranked by significance, with most significantly upregulated PRC2 target at top and most significantly downregulated at bottom. A number of the indicated upregulated genes have been implicated in oncogenesis, cancer cell stemness, proinvasion/metastasis, adhesion, and cytokine and/or hedgehog signaling, and two downregulated genes (*Bin1*, *Diras1*) encode tumor suppressors. **C**, RT-PCR analysis was performed on 13 of the 16 indicated genes (two shown here), validating the RNA-seq data in each instance. **D**, Immunoblot demonstrating overexpression of *Mmp9* and *Mmp2* in MMs from TKO mice (top). Top bands indicate respective pro-*Mmp9* and pro-*Mmp2*; bottom bands represent cleaved, active forms. Lysates were run on Novex 10% Zymogram gel and stained using colloidal blue staining kit to visualize *Mmp2/9* activity (bottom). **E**, Assessment of *BAP1*, *CDKN2A* and *NF2* in 87 human malignant mesotheliomas from TCGA. Seven malignant mesotheliomas (green open rectangle, designated DKO here) were null for both *CDKN2A* and *NF2*, and 6 (red open rectangle, designated TKO) were null for *BAP1*, *CDKN2A*, and *NF2*. **F**, Gene enrichment plots of several gene sets differentially expressed in TKO versus DKO human malignant mesotheliomas.

histology seen in human malignant mesotheliomas, as opposed to mice, may be the result of species-specific differences or route of induction, including the long latency and exposure to asbestos in the human disease counterpart (20). It is also likely that the particular mouse strain can influence the phenotype observed. For example, in our previous asbestos carcinogenesis work, *Nf2*^{+/-} mice in a 129Sv/Jae genetic background injected intraperitoneally with asbestos developed roughly equivalent percentages of epithelioid, mixed, and sarcomatoid malignant mesotheliomas (4), whereas asbestos-injected *Nf2*^{+/-} mice in a FVB/N background mostly developed sarcomatoid malignant mesotheliomas (21).

Heterozygous knockout (+/-) and heterozygous mutant (+/mut) *Bap1* mice injected intraperitoneally with asbestos exhibit a highly significant increase in the incidence of malignant mesotheliomas as compared with asbestos-injected WT littermates, providing *in vivo* evidence that *Bap1* inactivation plays an important role in malignant mesothelioma tumorigenesis (30, 31). Similarly, heterozygous *Nf2* mice injected with asbestos develop malignant mesothelioma with a markedly shorter latency than asbestos-treated WT littermates (4, 19). Heterozygous *Cdkn2a* knockout mice treated with asbestos also develop malignant mesothelioma at an accelerated rate compared with asbestos-treated WT mice (14). Furthermore, asbestos-exposed compound *Nf2*^{+/-};*Cdkn2a*^{+/-} mice show further acceleration of asbestos-induced malignant mesothelioma and increased presence of cancer stem cells (21). These carcinogenesis studies, in combination with the gene knockout model studies reported here strongly support a working hypothesis that *Bap1*, *Nf2*, and *Cdkn2a* are key drivers of malignant mesothelioma pathogenesis and that the collective losses of these three tumor suppressors is sufficient to drive rapidly disseminated, lethal disease, similar to the poor clinical outcome of human pleural malignant mesothelioma.

In one study, CKO mice in which only one of these tumor suppressor genes was homozygously deleted developed malignant mesothelioma at a low rate, with spontaneous malignant mesothelioma-like tumors being identified in 5 of 30 *Nf2*^{fl/fl} mice and 0 of 17 *Cdkn2a*^{fl/fl} mice injected intrathoracically with Adeno-Cre (20), supporting the notion that malignant mesothelioma development requires the combined involvement of multiple tumor suppressor gene alterations (42). Similarly, in our *Bap1* CKO cohort, malignant mesothelioma was seen in only 1 of 32 mice. The fact that malignant mesothelioma arises spontaneously in a considerable number of CKO mice made deficient for both alleles of two or more tumor suppressor genes, provides compelling support for the role of genetics in malignant mesothelioma causation and the need for accumulated genetic and epigenetic alterations for tumor formation (1). As an example, even in the one *Bap1* CKO mouse that did develop malignant mesothelioma, it is intriguing that there was acquired loss of *Nf2* and p16Ink4a expression during tumorigenesis.

The *in vivo* findings presented here with CKO mice closely mimic those found in the human disease counterpart, in which losses of *BAP1*, *CDKN2A*, and *NF2* are frequently seen in various combinations (7, 43). Their frequent occurrence in malignant mesothelioma and their individual roles both in various cancer predisposition syndromes and in tumor progression strongly suggest that they are key drivers in malignant mesothelioma pathogenesis. Our initial work on *BAP1* provided the first demonstration that genetics influences the risk of malignant mesothelioma, a cancer linked to mineral fiber carcinogenesis (8).

However, there is evidence that germline mutations of *CDKN2A* and *NF2* may also modulate susceptibility to mineral fiber carcinogens. For example, Betti and colleagues recently described a family in which both malignant mesothelioma and cutaneous melanoma cases were found to have a deleterious germline missense mutation in the *CDKN2A* gene, and the family member with malignant mesothelioma was determined to be of the low exposure category (44). In addition, germline mutations in *NF2* have been reported in patients who developed malignant mesothelioma. In one case, an individual with neurofibromatosis, type II (NF2) developed peritoneal malignant mesothelioma at the relatively young age of 40 (45). Comparative genomic hybridization analysis and IHC staining of the malignant mesothelioma tissue revealed loss of the *NF2* gene and protein product, respectively. A second NF2 patient developed a pleural malignant mesothelioma at the age of 75 years (46). Both patients were reported to have occupational asbestos exposure.

Our observation that CKO mice with losses of all three tumor suppressor genes had much higher malignant mesothelioma penetrance and markedly shorter survival than mice with loss of one or two of these genes fits with the model put forward by Vogelstein and Kinzler (47). They proposed that in solid tumors of adults, alterations in a minimum of three mutated driver genes are needed for a cell to evolve into an invasive (malignant) tumor. In our CKO models, loss of one or two tumor suppressors was not consistently sufficient to result in a high incidence of malignant mesotheliomas. The exception was the *Nf2*;*Cdkn2a* CKO model, but even in these mice tumor latency was much longer than in the triple-CKO mouse model. One possibility is that in *Nf2*;*Cdkn2a* CKO mice, significantly more time is needed to accumulate additional genetic and epigenetic alterations sufficient to result in an invasive cancer. In fact, 4 of 6 MMs tested from *Nf2*;*Cdkn2a* CKO mice acquired loss of *Bap1* expression (Fig. 4), suggesting that *Bap1* loss may be favored in the progression of these tumors. In human malignant mesothelioma, tumors are characterized by the presence of multiple somatic genetic and cell signaling alterations. The fact that large spheroids can be reproducibly formed *in vitro* in normal mesothelial cells following Adeno-Cre-induced excision of *Bap1*, *Cdkn2a* and *Nf2*, but not by the excision of only one or two of these genes, also provides experimental support for cooperativity between the inactivation of these three tumor suppressor genes in malignant mesothelioma tumorigenesis.

Our RNA-seq analysis revealed that malignant mesotheliomas from *Bap1*;*Nf2*;*Cdkn2a* CKO mice exhibit positively enriched gene sets consistent with cellular processes previously implicated in *Bap1* function, such as genes mediated by the *Bap1*-HCF1-YY1 complex, which play a role in cellular proliferation and transcription regulation involving ubiquitin signaling (25). In addition, in the experimental context used here, we have uncovered a connection between *Bap1* and PRC2 that has been less well established than other previously reported *Bap1*-related cellular activities.

Interestingly, a considerable number of upregulated genes in malignant mesotheliomas from triple-CKO mice have been implicated as oncogenes or proinvasion/metastasis genes, whereas several tumor suppressor genes were downregulated. Lafave and colleagues demonstrated that *BAP1* inactivation leads to *EZH2*-dependent transformation (48). Although their report did not include RNA-seq analysis on human malignant mesothelioma tumors for comparison with our murine data, they demonstrated that *BAP1*-deficient malignant mesothelioma cells are

sensitive to EZH2 pharmacologic inhibition, and our findings add support to their conclusion that such an approach may have clinical efficacy. It is noteworthy that PRC2 subunits such as Ezh2 have been shown to have context-dependent oncogenic or tumor-suppressive roles in different cancers (49).

To investigate whether our CKO mouse model findings are recapitulated in human malignant mesotheliomas with biallelic inactivation of *BAP1*, *CDKN2A*, and *NF2* versus malignant mesotheliomas with biallelic inactivation of *CDKN2A* and *NF2* only, we analyzed data from The Cancer Genome Atlas (TCGA; Supplementary Materials and Methods; Fig. 6E and F). GSEA analysis of the TCGA data revealed several positively enriched gene sets associated with SUZ12, PRC2, as well as EZH2 mediated trimethylation of H3K27 in human malignant mesotheliomas with biallelic inactivation of all three tumor suppressor genes (Fig. 6F; Supplementary Table S4), similar to the situation in malignant mesotheliomas from our TKO mice.

Mechanistically, our findings suggest that losses of *Bap1*, *Nf2*, and *Cdkn2a* cooperate by disrupting multiple cellular pathways that lead to the transformation of normal mesothelial cells to malignant mesothelioma cells. Thus, *Cdkn2a* loss would result in insensitivity to antigrowth signals (via p16Ink4a loss) and evasion of apoptosis (p19Arf loss), whereas *Nf2* loss would be expected to result in evasion of apoptosis and tissue invasion/metastasis (Hippo, Pak) and TAZ-related malignant mesothelioma cell transformation and transcriptional induction of distinct pro-oncogenic genes, including cytokines (50). On the basis of the upregulated genes identified in malignant mesotheliomas from TKO mice, other possible effects such as Lmo1-induced ECM and integrin-related self-sufficiency in growth signals, Aldh1a2- and Gli1-related maintenance of cancer stem cells, and Mmp9-induced invasiveness (Fig. 6D) may be mechanistically connected with *Bap1* inactivation and will be explored in future studies.

Collectively, *Bap1^{fl/fl};Nf2^{fl/fl};Cdkn2a^{fl/fl}* mice injected intrathoracically with Adeno-Cre appear to be useful for modeling an aggressive form of malignant mesothelioma. These malignant mesotheliomas develop at a high incidence after a short latency period. Moreover, our finding that loss of *Bap1* contributes to malignant mesothelioma pathogenesis, in part, via loss of PRC2-mediated repression of certain oncogenic target genes,

suggests a potential avenue for therapeutic intervention that may be rapidly tested in this CKO model.

Disclosure of Potential Conflicts of Interest

No potential conflicts of interest were disclosed.

Authors' Contributions

Conception and design: A.-M. Kukuyan, C.W. Menges, F.J. Rauscher, J.R. Testa
Development of methodology: A.-M. Kukuyan, Y. Kadariya, K.Q. Cai, F.J. Rauscher

Acquisition of data (provided animals, acquired and managed patients, provided facilities, etc.): A.-M. Kukuyan, E. Sementino, Y. Kadariya, C.W. Menges, Y. Tan, K.Q. Cai, S. Peri, A.J. Klein-Szanto

Analysis and interpretation of data (e.g., statistical analysis, biostatistics, computational analysis): A.-M. Kukuyan, Y. Kadariya, C.W. Menges, M. Cheung, K.Q. Cai, M.J. Slifker, S. Peri, A.J. Klein-Szanto, F.J. Rauscher, J.R. Testa

Writing, review, and/or revision of the manuscript: A.-M. Kukuyan, Y. Kadariya, C.W. Menges, S. Peri, F.J. Rauscher, J.R. Testa

Administrative, technical, or material support (i.e., reporting or organizing data, constructing databases): E. Sementino, M. Cheung

Study supervision: A.-M. Kukuyan, Y. Kadariya, J.R. Testa

Other (genotyped the mice to acquire the necessary arms for the experiment; checked mice for tumor development and acquired tumor samples used in the RNA-seq; performed spheroid assay; and obtained necessary Western blots): A.-M. Kukuyan

Acknowledgments

This work was supported by NCI grants CA175691 (to J.R. Testa and F.J. Rauscher III) and CA06927 (to FCCC) and an appropriation from the Commonwealth of Pennsylvania to FCCC. Other support was provided by the Local #14 Mesothelioma Fund of the International Association of Heat and Frost Insulators and Allied Workers. We thank Emmanuelle Nicolas for RT-PCR analyses, Eric Ross for statistical assistance, Alfonso Bellacosa for critical reading of the manuscript, and Raza Zaidi, Xavier Graña, Siddharth Balachandran, and Richard Pomerantz for scientific advice and technical suggestions. The following FCCC core services assisted this project: Laboratory Animal, Transgenic Mouse, Genomics, Cell Culture, DNA Sequencing, Histopathology, and Biostatistics and Bioinformatics Facilities.

The costs of publication of this article were defrayed in part by the payment of page charges. This article must therefore be hereby marked *advertisement* in accordance with 18 U.S.C. Section 1734 solely to indicate this fact.

Received January 2, 2019; revised May 1, 2019; accepted May 30, 2019; published first May 31, 2019.

References

- Murthy SS, Testa JR. Asbestos, chromosomal deletions, and tumor suppressor gene alterations in human malignant mesothelioma. *J Cell Physiol* 1999;180:150-7.
- Cheng JQ, Jhanwar SC, Klein WM, Bell DW, Lee W-C, Altomare DA, et al. *p16* alterations and deletion mapping of 9p21-p22 in malignant mesothelioma. *Cancer Res* 1994;54:5547-51.
- Xio S, Li D, Vijg J, Sugarbaker DJ, Corson JM, Fletcher JA. Codeletion of p15 and p16 in primary malignant mesothelioma. *Oncogene* 1995;11:511-5.
- Altomare DA, Vaslet CA, Skele KL, De Rienzo A, Devarajan K, Jhanwar SC, et al. A mouse model recapitulating molecular features of human mesothelioma. *Cancer Res* 2005;65:8090-5.
- Sekido Y, Pass HI, Bader S, Mew DJY, Christman MF, Gazdar AF, et al. Neurofibromatosis type 2 (*NF2*) gene is somatically mutated in mesothelioma but not in lung cancer. *Cancer Res* 1995;55:1227-31.
- Bianchi AB, Mitsunaga S-I, Cheng JQ, Klein WM, Jhanwar SC, Seizinger B, et al. High frequency of inactivating mutations in the neurofibromatosis type 2 gene (*NF2*) in primary malignant mesotheliomas. *Proc Natl Acad Sci U S A* 1995;92:10854-8.
- Bott M, Brevet M, Taylor BS, Shimizu S, Ito T, Wang L, et al. The nuclear deubiquitinase BAP1 is commonly inactivated by somatic mutations and 3p21.1 losses in malignant pleural mesothelioma. *Nat Genet* 2011;43:668-72.
- Testa JR, Cheung M, Pei J, Below JE, Tan Y, Sementino E, et al. Germline BAP1 mutations predispose to malignant mesothelioma. *Nat Genet* 2011;43:1022-5.
- Hmeljak J, Sanchez-Vega F, Hoadley KA, Shih J, Stewart C, Heiman D, et al. Integrative molecular characterization of malignant pleural mesothelioma. *Cancer Discov* 2018;8:1548-65.
- Cheng JQ, Lee WC, Klein MA, Cheng GZ, Jhanwar SC, Testa JR. Frequent mutations of *NF2* and allelic loss from chromosome band 22q12 in malignant mesothelioma: evidence for a two-hit mechanism of *NF2* inactivation. *Genes Chromosomes Cancer* 1999;24:238-42.
- Nasu M, Emi M, Pastorino S, Tanji M, Powers A, Luk H, et al. High incidence of somatic *BAP1* alterations in sporadic malignant mesothelioma. *J Thoracic Oncol* 2015;10:565-76.
- Frizelle SP, Grim J, Zhou J, Gupta P, Curiel DT, Geradts J, et al. Re-expression of p16INK4a in mesothelioma cells results in cell cycle arrest,

- cell death, tumor suppression and tumor regression. *Oncogene* 1998;16:3087–95.
13. Yang CT, You L, Yeh CC, Chang JW, Zhang F, McCormick F, et al. Adenovirus-mediated p14(ARF) gene transfer in human mesothelioma cells. *J Natl Cancer Inst* 2000;92:636–41.
 14. Altomare DA, Menges CW, Xu J, Pei J, Zhang L, Tadevosyan A, et al. Losses of both products of the *Cdkn2a/Arf* locus contribute to asbestos-induced mesothelioma development and cooperate to accelerate tumorigenesis. *PLoS One* 2011;6:e18828.
 15. Xiao GH, Gallagher R, Shetler J, Skele K, Altomare DA, Pestell RG, et al. The *NF2* tumor suppressor gene product, merlin, inhibits cell proliferation and cell cycle progression by repressing cyclin D1 expression. *Mol Cell Biol* 2005;25:2384–94.
 16. Lopez-Lago MA, Okada T, Murillo MM, Socci N, Giancotti FG. Loss of the tumor suppressor gene *NF2*, encoding merlin, constitutively activates integrin-dependent mTORC1 signaling. *Mol Cell Biol* 2009;29:4235–49.
 17. Xiao GH, Beeser A, Chernoff J, Testa JR. p21-activated kinase links *Rac/Cdc42* signaling to merlin. *J Biol Chem* 2002;277:883–6.
 18. Poulidakos PI, Xiao GH, Gallagher R, Jablonski S, Jhanwar SC, Testa JR. Re-expression of the tumor suppressor *NF2/merlin* inhibits invasiveness in mesothelioma cells and negatively regulates FAK. *Oncogene* 2006;25:5960–8.
 19. Fleury-Feith J, Lecomte C, Renier A, Matrat M, Kheuang L, Abramowski V, et al. Hemizyosity of *Nf2* is associated with increased susceptibility to asbestos-induced peritoneal tumours. *Oncogene* 2003;22:3799–805.
 20. Jongsma J, van Montfort E, Vooijs M, Zevenhoven J, Krimpenfort P, van der Valk M, et al. A conditional mouse model for malignant mesothelioma. *Cancer Cell* 2008;12:261–71.
 21. Menges CW, Kadariya Y, Altomare D, Talarchek J, Neumann-Domer E, Wu Y, et al. Tumor suppressor alterations cooperate to drive aggressive mesotheliomas with enriched cancer stem cells via a p53-miR-34a-c-Met axis. *Cancer Res* 2014;74:1261–71.
 22. Jensen DE, Proctor M, Marquis ST, Gardner HP, Ha SI, Chodosh LA, et al. BAP1: a novel ubiquitin hydrolase which binds to the BRCA1 RING finger and enhances BRCA1-mediated cell growth suppression. *Oncogene* 1998;16:1097–112.
 23. Scheuermann JC, de Ayala Alonso AG, Oktaba K, Ly-Hartig N, McGinty RK, Fraterman S, et al. Histone H2A deubiquitinase activity of the Polycomb repressive complex PR-DUB. *Nature* 2010;465:243–7.
 24. Misaghi S, Ottosen S, Izrael-Tomasevic A, Arnott D, Lamkanfi M, Lee J, et al. Association of C-terminal ubiquitin hydrolase BRCA1-associated protein 1 with cell cycle regulator host cell factor 1. *Mol Cell Biol* 2009;29:2181–92.
 25. Yu H, Mashtalir N, Daou S, Hammond-Martel I, Ross J, Sui G, et al. The ubiquitin carboxyl hydrolase BAP1 forms a ternary complex with YY1 and HCF-1 and is a critical regulator of gene expression. *Mol Cell Biol* 2010;30:5071–85.
 26. Yu H, Pak H, Hammond-Martel I, Ghram M, Rodrigue A, Daou S, et al. Tumor suppressor and deubiquitinase BAP1 promotes DNA double-strand break repair. *Proc Natl Acad Sci U S A* 2014;111:285–90.
 27. Baughman JM, Rose CM, Kolumam G, Webster JD, Wilkerson EM, Merrill AE, et al. NeuCode proteomics reveals Bap1 regulation of metabolism. *Cell Rep* 2016;16:583–95.
 28. Gezgin G, Dogrusoz M, van Essen TH, Kroes WGM, Luyten GPM, van der Velden PA, et al. Genetic evolution of uveal melanoma guides the development of an inflammatory microenvironment. *Cancer Immunol Immunother* 2017;66:903–12.
 29. Affar EB, Carbone M. BAP1 regulates different mechanisms of cell death. *Cell Death Dis* 2018;9:1151.
 30. Xu J, Kadariya Y, Cheung M, Pei J, Talarchek J, Sementino E, et al. Germline mutation of *Bap1* accelerates development of asbestos-induced malignant mesothelioma. *Cancer Res* 2014;74:4388–97.
 31. Napolitano A, Pellegrini L, Dey A, Larson D, Tanji M, Flores EG, et al. Minimal asbestos exposure in germline *BAP1* heterozygous mice is associated with deregulated inflammatory response and increased risk of mesothelioma. *Oncogene* 2016;35:1996–2002.
 32. Baumann F, Flores E, Napolitano A, Kanodia S, Taioli E, Pass H, et al. Mesothelioma patients with germline *BAP1* mutations have 7-fold improved long-term survival. *Carcinogenesis* 2015;36:76–81.
 33. Ohar JA, Cheung M, Talarchek J, Howard SE, Howard TD, Hesdorffer M, et al. Germline BAP1 Mutational landscape of asbestos-exposed malignant mesothelioma patients with family history of cancer. *Cancer Res* 2016;76:206–15.
 34. Harbour JW, Onken MD, Roberson ED, Duan S, Cao L, Worley LA, et al. Frequent mutation of *BAP1* in metastasizing uveal melanomas. *Science* 2010;330:1410–3.
 35. Pena-Llopis S, Vega-Rubin-de-Celis S, Liao A, Leng N, Pavia-Jimenez A, Wang S, et al. *BAP1* loss defines a new class of renal cell carcinoma. *Nat Genet* 2012;44:751–9.
 36. Bot J, Whitaker D, Vivian J, Lake R, Yao V, McCauley R. Culturing mouse peritoneal mesothelial cells. *Pathol Res Pract* 2003;199:341–4.
 37. Love MI, Huber W, Anders S. Moderated estimation of fold change and dispersion for RNA-seq data with DESeq2. *Genome Biol* 2014;15:550.
 38. Durinck S, Spellman PT, Birney E, Huber W. Mapping identifiers for the integration of genomic datasets with the R/Bioconductor package biomaRt. *Nat Protoc* 2009;4:1184–91.
 39. Subramanian A, Tamayo P, Mootha VK, Mukherjee S, Ebert BL, Gillette MA, et al. Gene set enrichment analysis: a knowledge-based approach for interpreting genome-wide expression profiles. *Proc Natl Acad Sci U S A* 2005;102:15545–50.
 40. Sashida G, Wang C, Tomioka T, Oshima M, Aoyama K, Kanai A, et al. The loss of *Ezh2* drives the pathogenesis of myelofibrosis and sensitizes tumor-initiating cells to bromodomain inhibition. *J Exp Med* 2016;213:1459–77.
 41. Benhamouche S, Curto M, Saotome I, Gladden AB, Liu CH, Giovannini M, et al. *NF2/Merlin* controls progenitor homeostasis and tumorigenesis in the liver. *Genes Dev* 2010;24:1718–30.
 42. Taguchi T, Jhanwar SC, Siegfried JM, Keller SM, Testa JR. Recurrent deletions of specific chromosomal sites in 1p, 3p, 6q, and 9p in human malignant mesothelioma. *Cancer Res* 1993;53:4349–55.
 43. Cheung M, Testa JR. *BAP1*, a tumor suppressor gene driving malignant mesothelioma. *Transl Lung Cancer Res* 2017;6:270–8.
 44. Betti M, Aspesi A, Biasi A, Casalone E, Ferrante D, Ogliara P, et al. *CDKN2A* and *BAP1* germline mutations predispose to melanoma and mesothelioma. *Cancer Lett* 2016;378:120–30.
 45. Baser ME, De Rienzo A, Altomare D, Balsara BR, Hedrick NM, Gutmann DH, et al. Neurofibromatosis 2 and malignant mesothelioma. *Neurology* 2002;59:290–1.
 46. Baser ME, Rai H, Wallace AJ, Evans DG. Neurofibromatosis 2 (NF2) and malignant mesothelioma in a man with a constitutional *NF2* missense mutation. *Fam Cancer* 2005;4:321–2.
 47. Vogelstein B, Kinzler KW. The path to cancer—three strikes and you're out. *N Engl J Med* 2015;373:1895–8.
 48. LaFave LM, Beguelin W, Koche R, Teater M, Spitzer B, Chramiec A, et al. Loss of BAP1 function leads to EZH2-dependent transformation. *Nat Med* 2015;21:1344–9.
 49. Vo BT, Li C, Morgan MA, Theurillat I, Finkelstein D, Wright S, et al. Inactivation of *Ezh2* upregulates *Gfi1* and drives aggressive Myc-driven group 3 medulloblastoma. *Cell Rep* 2017;18:2907–17.
 50. Matsushita A, Sato T, Mukai S, Fujishita T, Mishihiro-Sato E, Okuda M, et al. TAZ activation by Hippo pathway dysregulation induces cytokine gene expression and promotes mesothelial cell transformation. *Oncogene* 2019;38:1966–78.